

Exploring strong and weak topological states on isostructural substitutions in TlBiSe_2

Ankita Phutela,* Preeti Bhumla, Manjari Jain, and Saswata Bhattacharya*

Department of Physics, Indian Institute of Technology Delhi, New Delhi, India

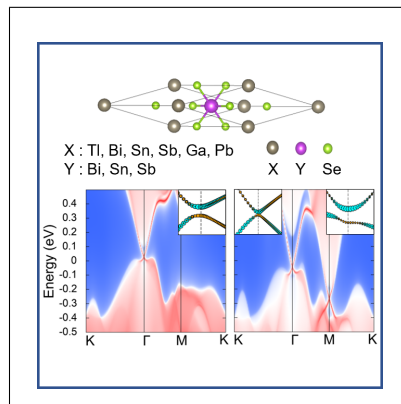
E-mail: Ankita@physics.iitd.ac.in[AP]; saswata@physics.iitd.ac.in[SB]

Phone: +91-11-2659 1359

Abstract

Topological Insulators (TIs) are unique materials where insulating bulk hosts linearly dispersing surface states protected by the Time-Reversal Symmetry (TRS). These states lead to dissipationless current flow, which makes this class of materials highly promising for spintronic applications. Here, we predict new TIs via high-throughput screening by employing state-of-the-art first-principles based methodologies, viz., Density Functional Theory (DFT) and many-body perturbation theory (G_0W_0) combined with Spin-Orbit Coupling (SOC). For this, we take a well-known 3D TI, TlBiSe₂ and perform complete substitution with suitable materials at different sites to check if the obtained isostructural materials exhibit topological properties. Subsequently, we scan these materials based on SOC-induced parity inversion at Time-Reversal Invariant Momenta (TRIM). Later, to confirm the topological nature of selected materials, we plot their surface states along with calculation of Z_2 invariants. Our results show that GaBiSe₂ is a Strong Topological Insulator (STI). Besides, we report six Weak Topological Insulators (WTIs) viz. PbBiSe₂, SnBiSe₂, SbBiSe₂, Bi₂Se₂, TlSnSe₂ and PbSbSe₂. We have further verified that all the reported TIs are dynamically stable showing all real phonon modes of vibration.

Graphical TOC Entry



Keywords

Topological Insulator, Surface States, Z_2 invariant, Spin-Orbit Coupling, DFT

Introduction

Since the discovery of Topological Insulators (TIs) about a decade ago, there has been an enormous increase in interest towards topological condensed matter systems¹⁻⁸. TIs show great potential applications in quantum computing and spintronics due to the insensitivity of the transport property towards non-magnetic perturbations^{7,9}. TIs also pave the way for realizing novel quantum phenomena such as Weyl semimetals¹⁰, Majorana-fermions¹¹ and Higgs mechanism¹². These alluring materials are insulating in bulk but support the flow of electrons on their surface. As a result, their surface consists of linear states that are protected by the Time-Reversal Symmetry (TRS)¹³. A necessary condition for the appearance of these states is the inversion of bands, which takes place at the Time-Reversal Invariant Momenta (TRIM) in the bulk Brillouin Zone (BZ)^{14,15}. The natural ordering of the energy levels forming the edges of the gap is inverted owing to the strong Spin-Orbit Coupling (SOC) associated with heavy elements. The topology of TRS invariant insulators is characterized by the Z_2 index, ν_0 , which can either be 0 or 1, depicting a topologically trivial or non-trivial phase, respectively. However, it has been recently reported that even when $\nu_0 = 0$, the system can show non-trivial characteristics¹⁶. Based on whether the material hosts odd or even number of Dirac cones in the electronic structure of its surface, TIs are further classified as Strong Topological Insulator (STI) having Z_2 invariant, $\nu_0 = 1$ or Weak Topological Insulator (WTI) with Z_2 invariant, $\nu_0 = 0$ ^{17,18}. Nevertheless, the complete characterization of 3D TIs requires a set of, in total, four Z_2 numbers: $(\nu_0; \nu_1 \nu_2 \nu_3)$. The indices ν_1 , ν_2 and ν_3 are called weak indices and are believed to be nonrobust quantities^{19,20}. Therefore, the calculation of surface states and Z_2 invariant give complete information about the topological nature of material.

First-principles calculations led to the prediction of a large number of 2D and 3D TIs²¹⁻²³. Among the various well established families of 3D TIs, Bi_2Se_3 and Bi_2Te_3 have been most widely studied for investigating topological states and their properties²⁴. Their crystal structures consist of quintuple layers held together by weak van der Waals (vdW) forces, providing natural cleavage planes without breaking strong bonds. The band structure calculations in Bi_2Se_3 have shown that the Dirac point of surface state lies close to the valence band maximum (VBM)²⁵. This leads to the

opening of electron scattering channel from surface states to bulk continuum states, and the topological transport regime begins to collapse. Therefore, there is a strong need for new materials with ideal and relatively isolated Dirac cones. A variety of candidates with non-trivial electronic states including HgTe²⁶, InAs²⁷, ternary tetramytes $\text{Ge}_m\text{Bi}_{2n}\text{Te}_{(m+3n)}$ ²⁸, half-Huesler compounds^{29–34}, LiAuSe honeycomb lattice³⁵, $\beta\text{-Ag}_2\text{Te}$ ³⁶ to non-centrosymmetric BiTeX (X=Cl, Br, I)^{37–39} have been suggested. Theoretical studies have shown that Tl-based ternary chalcogenides viz., TlSbTe₂, TlBiSe₂ and TlBiTe₂ are 3D TIs with a single Dirac cone surface state at the Γ point, which is well isolated from the bulk continuum^{40,41}. Tl-based materials have a 3D character because each Tl (Bi) layer is sandwiched between two Se layers with strong coupling between neighboring atomic layers instead of weak vdW forces as in Bi₂Se₃. The electronic structure of many Tl-based TIs, viz. TlAB₂ (A = Sb, Bi and B = Se, Te, S), have been investigated by Density Functional Theory (DFT) calculations^{15,42}. The role of surface termination has also been explored in TlBiSe₂ and TlBiTe₂⁴³. Following this the isostructural substitution of the above base material is been endeavoured to retain it's topological properties. For example, In-based compounds like InBiTe₂ and InSbTe₂, crystallizing in the TlBiSe₂ like crystal structure have been studied. Surprisingly, these materials lack the Dirac cone feature, which depicts their topologically trivial nature⁴⁴. Therefore, despite TlAB₂ (A = Sb, Bi and B = Se, Te, S) shows topologically non-trivial band structure, any other isostructural substitution to retain its topological nature is hitherto unknown.

Motivated with this idea, in this letter, we have explored the possibility of having new materials belonging to same class of ternary chalcogenides via a thorough isostructural substitutions. First, we have performed substitution at suitable sites of TlBiSe₂ and scanned for those materials whose band structure shows band inversion at odd/even number of TRIMs. After that, to determine the accurate band gap of TlBiSe₂, we have employed various exchange–correlation (ϵ_{xc}) functionals viz., PBE+SOC, HSE06+SOC, G_0W_0 @PBE+SOC and G_0W_0 @HSE06+SOC. The band gap obtained from G_0W_0 @PBE+SOC functional is in close agreement with the experimental value. Therefore, we have further calculated the band gap of all materials using G_0W_0 @PBE+SOC. Subsequently, we have examined the potential materials for their dynamical stability. The stable ma-

materials are then characterised as STI/WTI depending on whether they show odd/even number of surface states, respectively. To confirm their topological nature, we have also calculated the Z_2 topological invariants.

TlBiSe₂ belongs to the TI-family of compounds having a rhombohedral crystal structure with space group $R\bar{3}m$ ^{40,41}. There are four atoms in the primitive unit cell which are placed in layers normal to the three-fold axis with the sequence -Tl-Se-Bi-Se-, i.e., along [111] axis of rhombohedral unit cell (see Figure 1(a)). The 3D BZ for rhombohedral unit cell having high symmetry points F, Γ , L and Z, along with its projected (111) surface BZ is shown in Figure 1(b). The structure has inversion symmetry where both Bi and Tl act as inversion centers. We have first estimated the band gap of TlBiSe₂ using PBE+SOC. The calculated band gap is 215 meV (Direct), whereas, the experimental band gap is 350 meV⁴⁵. The band gap is thus underestimated due to the DFT limitation arising from the approximations used in the ϵ_{xc} functional. Therefore, we have used hybrid ϵ_{xc} functional (HSE06) with default $\alpha = 0.25$, i.e., incorporating 25% of Hartree-Fock exact exchange to capture the electron's self-interaction error along with SOC. It gives a direct band gap of 85 meV, which is also not in accordance with previously reported theoretical calculations⁴³. Therefore, we have performed G_0W_0 calculations on top of the orbitals obtained from the PBE+SOC ($G_0W_0@PBE+SOC$) and HSE06+SOC ($G_0W_0@HSE06+SOC$). The respective band gaps are 280 meV and 249 meV (see Table 1). $G_0W_0@PBE+SOC$ gives the most accurate band gap, however, the band profile is not much affected by the choice of ϵ_{xc} functional (see Section I of Supplementary Information (SI)). Therefore, we have used PBE ϵ_{xc} functional to plot the band structures in view of its low computational cost. The band structure of TlBiSe₂ with the projected wavefunctions to atomic orbitals is shown in Figure 2(a). The Conduction Band (CB) is dominated by Bi-*p* and Tl-*p* orbitals, while Se-*p* orbitals dominate the Valence Band (VB). The inclusion of SOC has led to an increase in the band gap around the Γ point. The valence and conduction band edges switch their orbital character around this point, indicating the band inversion. The *p* orbitals of Se and Bi are involved in this band inversion, as can be clearly seen from Figure 2(b).

The similar band inversion has also been observed in TlBiTe₂ and TlSbSe₂⁴³. Following the

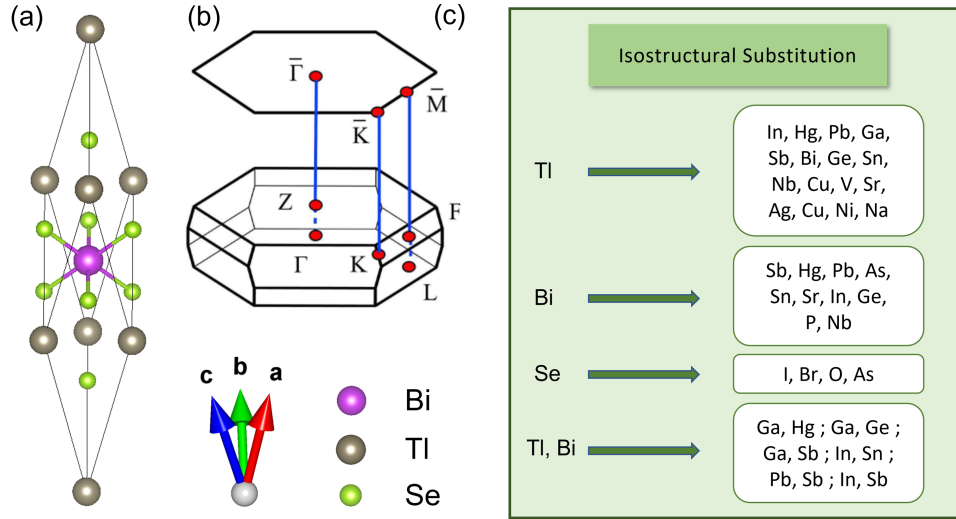


Figure 1: (a) Primitive crystal structure of TlBiSe₂, (b) 3D BZ for primitive unit cell with four time-reversal invariant points Γ , Z, F and L along with the projected surface BZ, and (c) Complete substitution with various elements at Tl, Bi, Se and Tl, Bi sites simultaneously.

Table 1: Band gap (in meV) of TlBiSe₂ using different ϵ_{xc} functionals.

PBE+SOC	HSE06+SOC	G ₀ W ₀ @PBE+SOC	G ₀ W ₀ @HSE06+SOC
215	85	280	249

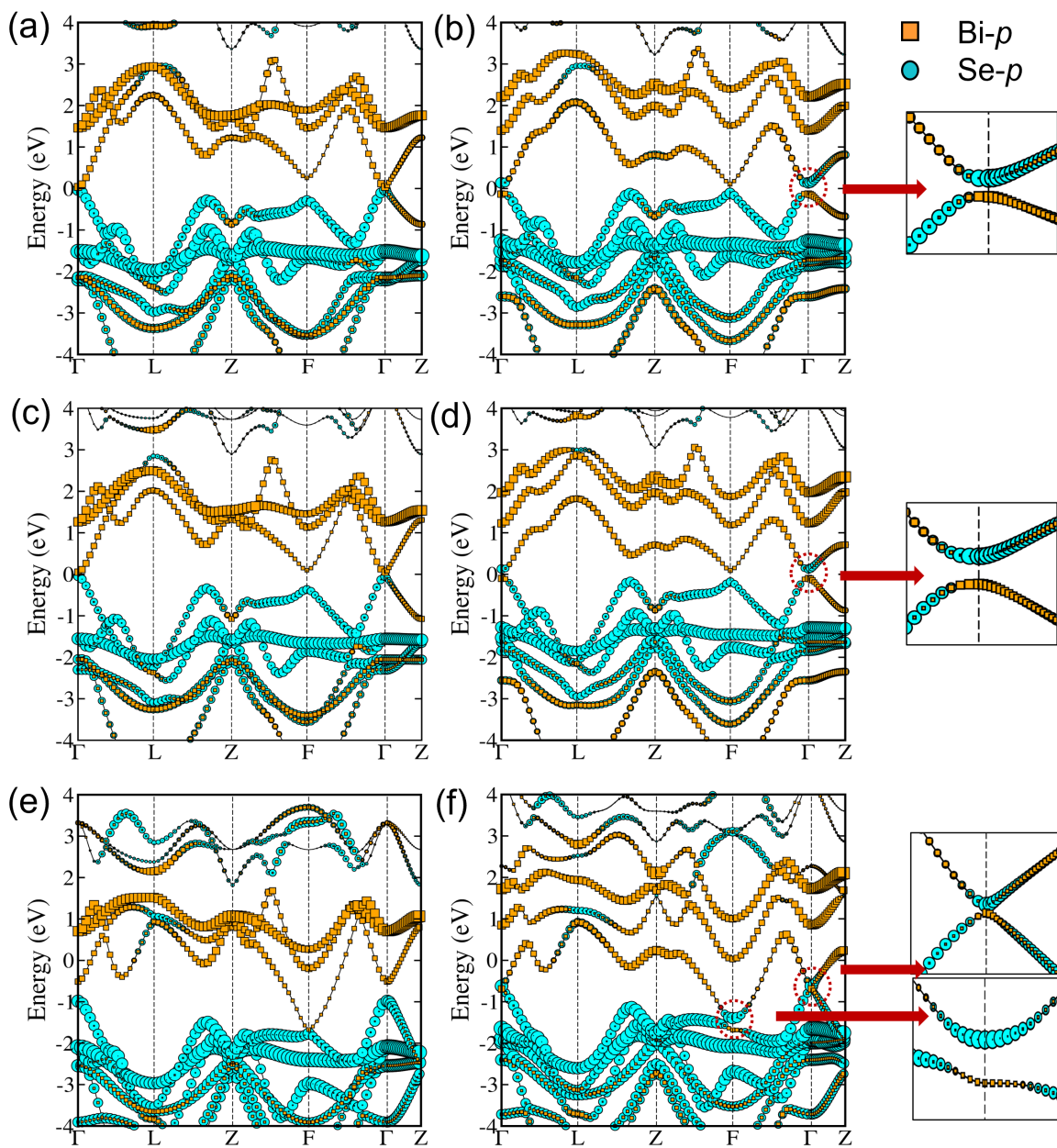


Figure 2: The band structures for TlBiSe_2 , GaBiSe_2 and PbBiSe_2 without SOC are shown in (a), (c), (e) and with SOC are shown in (b), (d), (f), respectively. Insets show band inversion at respective k -points.

trend, we have carried out complete substitution in TlBiSe₂ at Tl, Bi or Se sites and Tl, Bi sites simultaneously to obtain different materials belonging to the same class (see Figure 1(c)). The band structure of these materials are plotted to see the effect of SOC on the orbital contribution projected on the bands lying near Fermi level. Firstly, Ga is substituted at the Tl site (Ga_{Tl}) to form GaBiSe₂. It also crystallizes in $R\bar{3}m$ phase with lattice parameters given as $a = b = c = 7.18 \text{ \AA}$ (in rhombohedral setting) and yields the band structure shown in Figure 2(c). SOC driven inversion of energy levels along with opening of band gap takes place at high symmetry point Γ (Figure 2(d)). The projected wavefunctions to atomic orbitals show that p orbitals of all atoms contribute near the Fermi level. The inversion involves Bi- p and Se- p orbitals (similar to the case of TlBiSe₂), giving an initial indication that the material can harbor non-trivial topological phase. The indirect band gap as calculated by $G_0W_0@PBE+SOC$ is 183 meV.

Table 2: Band gap (in meV) of different materials using $G_0W_0@PBE+SOC$.

Material	Indirect Band Gap
GaBiSe ₂	183
PbBiSe ₂	3
SnBiSe ₂	20
SbBiSe ₂	118
Bi ₂ Se ₂	327
TlSnSe ₂	44
PbSbSe ₂	41

After GaBiSe₂, we have substituted Pb_{Tl} to get PbBiSe₂ having lattice parameters as $a = b = c = 8.27 \text{ \AA}$, and crystallizing in the $R\bar{3}m$ phase. $G_0W_0@PBE+SOC$ yields an indirect band gap of 3 meV. The VB and CB are mainly composed of p orbitals of Pb, Bi and Se, as shown in Figure 2(e) and 2(f). The parity inversion occurs at Γ and F points, unlike the former. In this BZ, there are 8 TRIMs, i.e., Γ , Z (non-degenerate) and F, L (triply-degenerate). Therefore, the inversion is occurring at even number of TRIMs, which means that the system should be in trivial state. However, it has been found that if even number of band inversions occur in the first quadrant, but if one or more BZ sides possess odd number of band inversions, then a WTI can be obtained²¹.

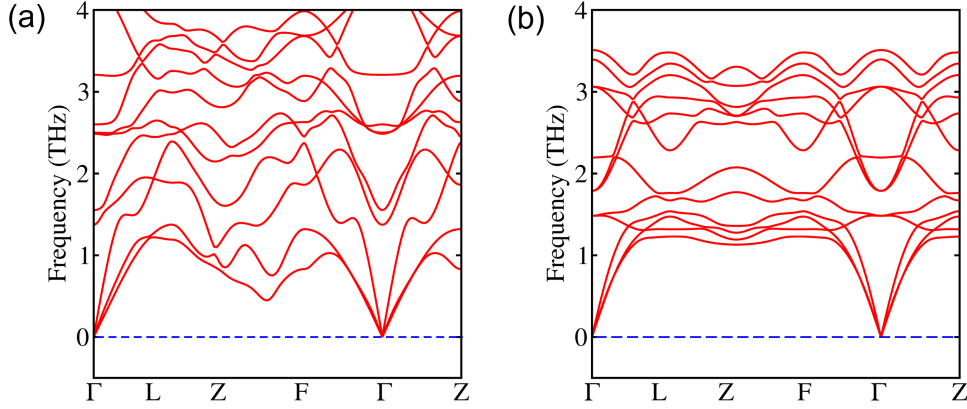


Figure 3: Phonon band structures of (a) GaBiSe₂ and (b) PbBiSe₂.

A similar type of parity inversion at even number of TRIMs is obtained for SnBiSe₂, SbBiSe₂, Bi₂Se₂, TlSnSe₂ and PbSbSe₂ (refer Section II and Section III of SI for band structures and optimized lattice parameters, respectively). The band gap of all these materials calculated using G₀W₀@PBE+SOC are given in Table 2. After screening the systems for SOC-induced inversion in the band structures, we have analyzed them for dynamical stability. Figure 3 shows the phonon band structures for GaBiSe₂ and PbBiSe₂. The absence of negative frequencies confirms the dynamical stability of these materials. For other systems viz. SnBiSe₂, SbBiSe₂, Bi₂Se₂, TlSnSe₂ and PbSbSe₂, see Section IV of SI.

The presence of band inversion on inclusion of SOC is a telltale signature of possibility of non-trivial phase. However, an inverted band structure cannot be considered as a sole criterion to assure the existence of a non-trivial phase. Therefore, further analysis is required to establish its topological nature. Previous studies have reported that non-trivial band topology generates metallic surface states which are the hallmark of TIs⁴⁶. In view of this, we have computed the spectrum of surface states by considering a semi infinite slab of 3D material. These lattice surfaces possess Dirac cones, lying at the same k -point where the band inversion has occurred in the corresponding bulk band structure. Furthermore, to elucidate the topological nature of the materials, Z_2 topological invariants are calculated. TRS yields four distinct Z_2 invariants ($\nu_0; \nu_1 \nu_2 \nu_3$) in 3D case. Each of these four invariants takes up value either 0 or 1, indicating a total of 16 phases with three general

classes: a normal insulator, a STI and a WTI²⁰. An ordinary or trivial insulator is obtained when all four invariants are zero, i.e., (0;000), while a STI is obtained when $\nu_0 = 1$. This type of system is robust against weak time-reversal invariant perturbations. However, when $\nu_0 = 0$, and at least one of the indices out of ν_1 , ν_2 or ν_3 is nonzero, then the material is WTI. It can be viewed as a stacking of 2D TIs, and is less robust against perturbations.

Table 3: Calculated Z_2 invariants for different materials.

Material	$Z_2:(\nu_0;\nu_1\nu_2\nu_3)$	Number of surface states	Type
GaBiSe₂	(1;000)	1	STI
PbBiSe₂	(0;001)	2	WTI
SnBiSe₂	(0;001)	2	WTI
SbBiSe₂	(0;001)	2	WTI
Bi₂Se₂	(0;001)	2	WTI
TlSnSe₂	(0;001)	2	WTI
PbSbSe₂	(0;111)	2	WTI

It has already been established that TlBiSe₂ is a strong 3D TI⁴⁷, on that account, we first obtain its surface band structure. For this, a tight-binding Hamiltonian with MLWFs considering the projection of p orbitals of Bi/Se and sp orbitals of Tl is constructed. Since the left and right surface for TlBiSe₂ terminates with different atoms (Tl and Se, respectively), therefore, we have plotted surface state spectra of (111) surface for both the surface terminations. Figure 4(a) and 4(b) show a single surface state protected by TRS at the Γ point in the projected 2D BZ. Alongside, we have calculated the topological invariant, ν_0 , which comes out to be 1, confirming that TlBiSe₂ is a STI. Following this, we have explored GaBiSe₂ for topological properties. In this case, the p orbitals of Bi/Se and sp orbitals of Ga are considered in constructing the tight-binding Hamiltonian. A single Dirac cone protected by TRS has been observed for (111) surface (see Figure 4(c) and 4(d)), and the corresponding topological invariant is (1;000), which is a signature of non-trivial topology. Hence, to the best of our knowledge, we report here GaBiSe₂ to be a STI presumably for the first time.

Afterwards, we have performed surface band structure calculation for PbBiSe₂. We have ob-

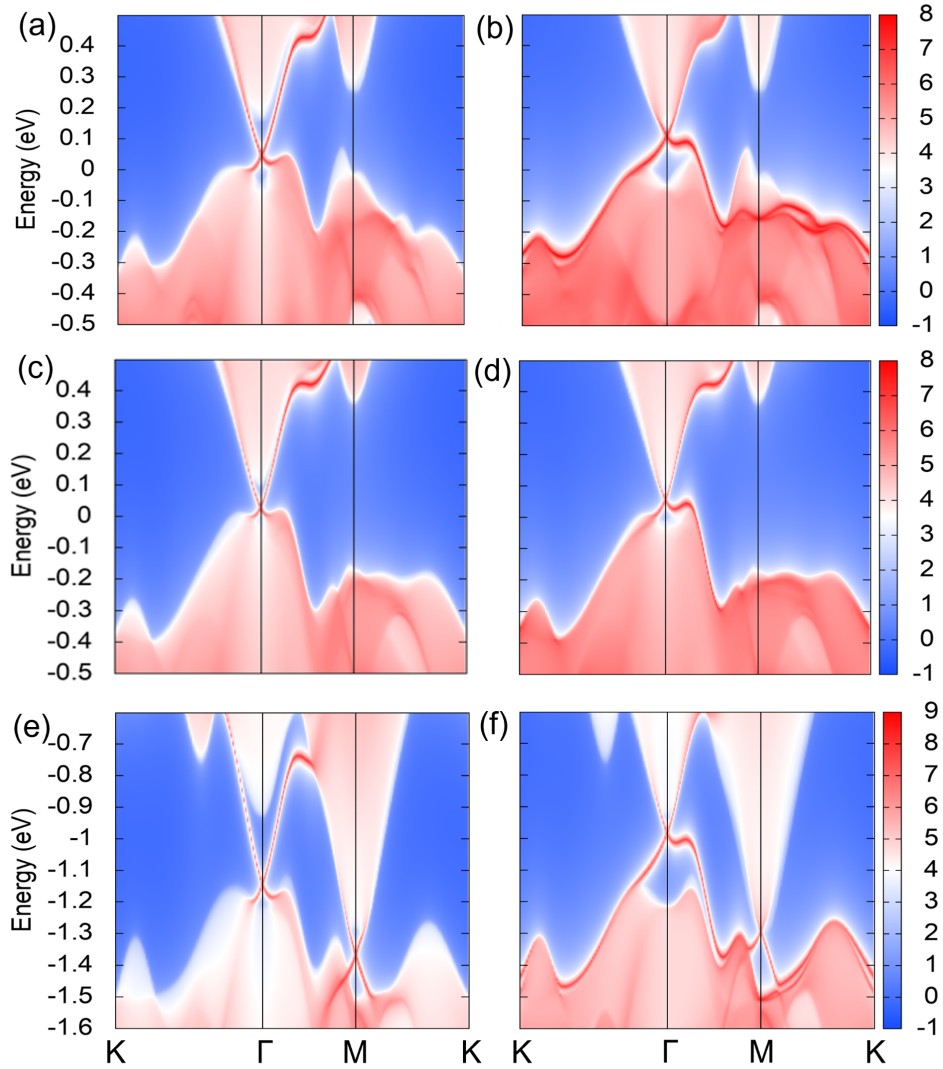


Figure 4: Surface states for the left surface of TlBiSe_2 , GaBiSe_2 and PbBiSe_2 are shown in (a), (c), (e) and for the right surface are shown in (b), (d), (f), respectively. Here, the sharp red curves represent surface states, whereas, the shaded regions show the spectral weight of projected bulk bands.

tained even (two) number of surface states lying at Γ and M (see Figure 4(e) and 4(f)). The presence of even number of surface states yields $\nu_0 = 0$, and the weak indices come out to be $\nu_1 = 0$, $\nu_2 = 0$ and $\nu_3 = 1$. As even number of surface states lead to scattering and thus are not topologically protected, hence this material is categorized as a WTI. The similar calculations are performed for SnBiSe₂, SbBiSe₂, Bi₂Se₂, TlSnSe₂ and PbSbSe₂. All of them show even number of surface states, as shown in Section V of SI, and corresponding Z_2 invariants are given in Table 3. These materials belong to the class of Z_2 WTI. Nowadays, WTIs are also getting attention as it has been found that their surface states are robust against imperfections, owing to the delocalization of surface electrons⁴⁸.

In summary, we have performed isostructural substitutions of materials based on SOC-induced parity inversion in the band structure. Using first-principles based methodologies, viz., PBE, HSE06, and many-body perturbation theory (G_0W_0), we have systematically studied the electronic structure of topological materials belonging to $R\bar{3}m$ space group. The band gap calculated using $G_0W_0@PBE+SOC$ is in close agreement with the experimental value. We have revealed that GaBiSe₂ is a STI as its surface accommodates a single crossing at the Γ point. PbBiSe₂, SnBiSe₂, SbBiSe₂, Bi₂Se₂, TlSnSe₂ and PbSbSe₂ are WTI catering even number of surface states within the bulk band gap. The absence of negative frequencies in the phonon band structures indicates dynamical stability. The calculated Z_2 invariants are in accordance with the surface state plots confirming their topological nature. Discovery of these materials will offer a great platform for studying novel quantum effects.

Computational Methods

The calculations are performed using DFT^{49,50} with the Projected Augmented Wave (PAW)^{51,52} method implemented in Vienna *Ab initio* Simulation Package (VASP)⁵³ code. All the structures are optimized with the Generalized Gradient Approximation (GGA) of Perdew-Burke-Ernzerhof (PBE)⁵⁴ until the Hellmann-Feynman forces are smaller than 0.001 eV/Å. The plane wave basis is

used with 400 eV cutoff energy. The Γ -centered $6\times 6\times 4$ k -grid is used to sample the irreducible BZ of rhombohedral phase with the $R\bar{3}m$ space group. SOC is included in all calculations except in ionic optimization. The advanced hybrid ϵ_{xc} functional (HSE06) including SOC and many-body perturbation methods, $G_0W_0@PBE+SOC$ and $G_0W_0@HSE06+SOC$ are used for the better estimation of the band gap⁵⁵. For this, we have used $4\times 4\times 4$ k -grid, and the number of bands is set to six times the number of occupied bands. The phonon calculations are performed with $4\times 4\times 4$ supercells using the PHONOPY package^{56,57}. In order to investigate the topological properties of the materials, we have performed DFT calculations using fully relativistic norm-conserving pseudopotentials as implemented in the QUANTUM ESPRESSO code⁵⁸. The results of these DFT calculations are then fed as input to WANNIER90⁵⁹ for constructing a tight-binding model based on Maximally Localized Wannier Functions (MLWFs) with p orbitals of Se, Bi and sp orbitals of Ga, Tl, Sn, Sb, Pb. The surface states and topological invariants are then calculated using the Green's function method as implemented in the Wannier-TOOLS package⁶⁰.

Acknowledgement

A.P. acknowledges IIT Delhi for the junior research fellowship. P.B. acknowledges UGC, India, for the senior research fellowship [Grant no. 1392/(CSIR-UGC NET JUNE 2018)]. M.J. acknowledges CSIR, India, for the senior research fellowship [Grant No. 09/086(1344)/2018-EMR-I]. S.B. acknowledges financial support from SERB under a core research grant (grant no. CRG/2019/000647) to set up his High Performance Computing (HPC) facility "Veena" at IIT Delhi for computational resources.

Supporting Information Available

Band profile of TlBiSe₂ using PBE+SOC and $G_0W_0@PBE+SOC$ ϵ_{xc} functionals; Band structures of SnBiSe₂, SbBiSe₂, Bi₂Se₂, TlSnSe₂ and PbSbSe₂; Optimized lattice parameters of SnBiSe₂, SbBiSe₂, Bi₂Se₂, TlSnSe₂ and PbSbSe₂; Phonon band structures of SbBiSe₂, SnBiSe₂, Bi₂Se₂,

TlSnSe₂ and PbSbSe₂; Surface state band structures of SnBiSe₂, SbBiSe₂, Bi₂Se₂, TlSnSe₂ and PbSbSe₂; Band gap (in meV) of different materials using G₀W₀@HSE06+SOC ϵ_{xc} functional.

References

- (1) Qi, X.-L.; Hughes, T. L.; Zhang, S.-C. Topological field theory of time-reversal invariant insulators. *Physical Review B* **2008**, *78*, 195424.
- (2) Moore, J. E.; Balents, L. Topological invariants of time-reversal-invariant band structures. *Physical Review B* **2007**, *75*, 121306.
- (3) Hasan, M. Z.; Kane, C. L. Colloquium: topological insulators. *Reviews of modern physics* **2010**, *82*, 3045.
- (4) Moore, J. E. The birth of topological insulators. *Nature* **2010**, *464*, 194–198.
- (5) Fu, L.; Kane, C. L.; Mele, E. J. Topological insulators in three dimensions. *Physical review letters* **2007**, *98*, 106803.
- (6) Bernevig, B. A.; Zhang, S.-C. Quantum spin Hall effect. *Physical review letters* **2006**, *96*, 106802.
- (7) Qi, X.-L.; Zhang, S.-C. Topological insulators and superconductors. *Reviews of Modern Physics* **2011**, *83*, 1057.
- (8) Hsieh, D.; Xia, Y.; Qian, D.; Wray, L.; Dil, J.; Meier, F.; Osterwalder, J.; Patthey, L.; Checkelsky, J.; Ong, N. P. et al. A tunable topological insulator in the spin helical Dirac transport regime. *Nature* **2009**, *460*, 1101–1105.
- (9) Wan, X.; Turner, A. M.; Vishwanath, A.; Savrasov, S. Y. Topological semimetal and Fermi-arc surface states in the electronic structure of pyrochlore iridates. *Physical Review B* **2011**, *83*, 205101.

- (10) Singh, B.; Sharma, A.; Lin, H.; Hasan, M.; Prasad, R.; Bansil, A. Topological electronic structure and Weyl semimetal in the TlBiSe₂ class of semiconductors. *Physical Review B* **2012**, *86*, 115208.
- (11) Wilczek, F. Majorana returns. *Nature Physics* **2009**, *5*, 614–618.
- (12) Sato, T.; Segawa, K.; Kosaka, K.; Souma, S.; Nakayama, K.; Eto, K.; Minami, T.; Ando, Y.; Takahashi, T. Unexpected mass acquisition of Dirac fermions at the quantum phase transition of a topological insulator. *Nature Physics* **2011**, *7*, 840–844.
- (13) Kane, C. L.; Mele, E. J. Z₂ topological order and the quantum spin Hall effect. *Physical review letters* **2005**, *95*, 146802.
- (14) Eremeev, S.; Koroteev, Y. M.; Chulkov, E. V. Ternary thallium-based semimetal chalcogenides Tl_{1-x}V_xVI₂ as a new class of three-dimensional topological insulators. *JETP letters* **2010**, *91*, 594–598.
- (15) Singh, B.; Lin, H.; Prasad, R.; Bansil, A. Topological phase transition and quantum spin Hall state in TlBiS₂. *Journal of applied physics* **2014**, *116*, 033704.
- (16) Lee, K.; Lange, G. F.; Wang, L.-L.; Kuthanazhi, B.; Trevisan, T. V.; Jo, N. H.; Schruck, B.; Orth, P. P.; Slager, R.-J.; Canfield, P. C. et al. Discovery of a weak topological insulating state and van Hove singularity in triclinic RhBi₂. *Nature communications* **2021**, *12*, 1–8.
- (17) Rusinov, I. P.; Menshchikova, T. V.; Isaeva, A.; Eremeev, S.; Koroteev, Y. M.; Vergniory, M.; Echenique, P. M.; Chulkov, E. V. Mirror-symmetry protected non-TRIM surface state in the weak topological insulator Bi₂TeI. *Scientific reports* **2016**, *6*, 1–7.
- (18) Majhi, K.; Pal, K.; Lohani, H.; Banerjee, A.; Mishra, P.; Yadav, A. K.; Ganesan, R.; Sekhar, B.; Waghmare, U. V.; Anil Kumar, P. Emergence of a weak topological insulator from the Bi_xSe_y family. *Applied Physics Letters* **2017**, *110*, 162102.

- (19) Imura, K.-I.; Takane, Y.; Tanaka, A. Weak topological insulator with protected gapless helical states. *Physical Review B* **2011**, *84*, 035443.
- (20) Noguchi, R.; Takahashi, T.; Kuroda, K.; Ochi, M.; Shirasawa, T.; Sakano, M.; Bareille, C.; Nakayama, M.; Watson, M.; Yaji, K. et al. A weak topological insulator state in quasi-one-dimensional bismuth iodide. *Nature* **2019**, *566*, 518–522.
- (21) Das, T. A pedagogic review on designing model topological insulators. *arXiv preprint arXiv:1604.07546* **2016**,
- (22) Hsieh, T. H.; Lin, H.; Liu, J.; Duan, W.; Bansil, A.; Fu, L. Topological crystalline insulators in the SnTe material class. *Nature communications* **2012**, *3*, 1–7.
- (23) Kou, L.; Ma, Y.; Sun, Z.; Heine, T.; Chen, C. Two-dimensional topological insulators: Progress and prospects. *The journal of physical chemistry letters* **2017**, *8*, 1905–1919.
- (24) Zhang, H.; Liu, C.-X.; Qi, X.-L.; Dai, X.; Fang, Z.; Zhang, S.-C. Topological insulators in Bi₂Se₃, Bi₂Te₃ and Sb₂Te₃ with a single Dirac cone on the surface. *Nature physics* **2009**, *5*, 438–442.
- (25) Reid, T. K.; Alpay, S. P.; Balatsky, A. V.; Nayak, S. K. First-principles modeling of binary layered topological insulators: Structural optimization and exchange-correlation functionals. *Physical Review B* **2020**, *101*, 085140.
- (26) Brüne, C.; Liu, C.; Novik, E.; Hankiewicz, E.; Buhmann, H.; Chen, Y.; Qi, X.; Shen, Z.; Zhang, S.; Molenkamp, L. Quantum Hall effect from the topological surface states of strained bulk HgTe. *Physical Review Letters* **2011**, *106*, 126803.
- (27) Lin, H.; Das, T.; Wang, Y. J.; Wray, L.; Xu, S.-Y.; Hasan, M.; Bansil, A. Adiabatic transformation as a search tool for new topological insulators: Distorted ternary Li₂AgSb-class semiconductors and related compounds. *Physical Review B* **2013**, *87*, 121202.

- (28) Lin, H.; Wray, L. A.; Xia, Y.; Xu, S.; Jia, S.; Cava, R.; Bansil, A.; Hasan, M. Z. *Nature Mater.* **9**, 546 (2010).
- (29) Lin, H.; Wray, L. A.; Xia, Y.; Xu, S.; Jia, S.; Cava, R. J.; Bansil, A.; Hasan, M. Z. Half-Heusler ternary compounds as new multifunctional experimental platforms for topological quantum phenomena. *Nature materials* **2010**, *9*, 546–549.
- (30) Chadov, S.; Qi, X.; Kübler, J.; Fecher, G. H.; Felser, C.; Zhang, S. C. Tunable multifunctional topological insulators in ternary Heusler compounds. *Nature materials* **2010**, *9*, 541–545.
- (31) Feng, W.; Xiao, D.; Zhang, Y.; Yao, Y. Half-Heusler topological insulators: A first-principles study with the Tran-Blaha modified Becke-Johnson density functional. *Physical Review B* **2010**, *82*, 235121.
- (32) Xiao, D.; Yao, Y.; Feng, W.; Wen, J.; Zhu, W.; Chen, X.-Q.; Stocks, G. M.; Zhang, Z. Half-Heusler compounds as a new class of three-dimensional topological insulators. *Physical review letters* **2010**, *105*, 096404.
- (33) Shitade, A.; Katsura, H.; Kuneš, J.; Qi, X.-L.; Zhang, S.-C.; Nagaosa, N. Quantum spin Hall effect in a transition metal oxide Na_2IrO_3 . *Physical review letters* **2009**, *102*, 256403.
- (34) Chadov, S.; Qi, X. J. Kübler, GH Fecher, C. Felser, SC Zhang. *Nat. Mater* **2010**, *9*, 541.
- (35) Zhang, H.-J.; Chadov, S.; Mühler, L.; Yan, B.; Qi, X.-L.; Kübler, J.; Zhang, S.-C.; Felser, C. Topological insulators in ternary compounds with a honeycomb lattice. *Physical review letters* **2011**, *106*, 156402.
- (36) Lee, S.; In, J.; Yoo, Y.; Jo, Y.; Park, Y. C.; Kim, H.-j.; Koo, H. C.; Kim, J.; Kim, B.; Wang, K. L. Single crystalline β - Ag_2Te nanowire as a new topological insulator. *Nano letters* **2012**, *12*, 4194–4199.
- (37) Chen, Y.; Kanou, M.; Liu, Z.; Zhang, H.; Sobota, J.; Leuenberger, D.; Mo, S.; Zhou, B.;

- Yang, S.; Kirchmann, P. et al. Discovery of a single topological Dirac fermion in the strong inversion asymmetric compound BiTeCl. *Nature Physics* **2013**, *9*, 704–708.
- (38) Landolt, G.; Ereemeev, S. V.; Tereshchenko, O. E.; Muff, S.; Slomski, B.; Kokh, K. A.; Kobayashi, M.; Schmitt, T.; Strocov, V. N.; Osterwalder, J. et al. Bulk and surface Rashba splitting in single termination BiTeCl. *New Journal of Physics* **2013**, *15*, 085022.
- (39) Bahramy, M.; Yang, B.-J.; Arita, R.; Nagaosa, N. Emergence of non-centrosymmetric topological insulating phase in BiTeI under pressure. *Nature communications* **2012**, *3*, 1–7.
- (40) Lin, H.; Markiewicz, R.; Wray, L.; Fu, L.; Hasan, M.; Bansil, A. Single-Dirac-cone topological surface states in the TlBiSe₂ class of topological semiconductors. *Physical review letters* **2010**, *105*, 036404.
- (41) Yan, B.; Liu, C.-X.; Zhang, H.-J.; Yam, C.-Y.; Qi, X.-L.; Frauenheim, T.; Zhang, S.-C. Theoretical prediction of topological insulators in thallium-based III-V-VI₂ ternary chalcogenides. *EPL (Europhysics Letters)* **2010**, *90*, 37002.
- (42) Zhang, Q.; Cheng, Y.; Schwingenschlögl, U. Emergence of topological and topological crystalline phases in TlBiS₂ and TlSbS₂. *Scientific reports* **2015**, *5*, 1–7.
- (43) Singh, B.; Lin, H.; Prasad, R.; Bansil, A. Role of surface termination in realizing well-isolated topological surface states within the bulk band gap in TlBiSe₂ and TlBiTe₂. *Physical Review B* **2016**, *93*, 085113.
- (44) Ereemeev, S.; Bihlmayer, G.; Vergniory, M.; Koroteev, Y. M.; Menshchikova, T. V.; Henk, J.; Ernst, A.; Chulkov, E. V. Ab initio electronic structure of thallium-based topological insulators. *Physical Review B* **2011**, *83*, 205129.
- (45) Sato, T.; Segawa, K.; Guo, H.; Sugawara, K.; Souma, S.; Takahashi, T.; Ando, Y. Direct evidence for the Dirac-cone topological surface states in the ternary chalcogenide TlBiSe₂. *Physical review letters* **2010**, *105*, 136802.

- (46) Hsieh, D.; Qian, D.; Wray, L.; Xia, Y.; Hor, Y. S.; Cava, R. J.; Hasan, M. Z. A topological Dirac insulator in a quantum spin Hall phase. *Nature* **2008**, *452*, 970–974.
- (47) Kuroda, K.; Ye, M.; Kimura, A.; Ereemeev, S.; Krasovskii, E.; Chulkov, E.; Ueda, Y.; Miyamoto, K.; Okuda, T.; Shimada, K. et al. Experimental realization of a three-dimensional topological insulator phase in ternary chalcogenide TlBiSe₂. *Physical review letters* **2010**, *105*, 146801.
- (48) Ringel, Z.; Kraus, Y. E.; Stern, A. Strong side of weak topological insulators. *Physical Review B* **2012**, *86*, 045102.
- (49) Hohenberg, P.; Kohn, W. Inhomogeneous electron gas. *Physical review* **1964**, *136*, B864.
- (50) Kohn, W.; Sham, L. J. Self-consistent equations including exchange and correlation effects. *Physical review* **1965**, *140*, A1133.
- (51) Kresse, G.; Joubert, D. From ultrasoft pseudopotentials to the projector augmented-wave method. *Physical review b* **1999**, *59*, 1758.
- (52) Blöchl, P. E. Projector augmented-wave method. *Physical review B* **1994**, *50*, 17953.
- (53) Kresse, G.; Furthmüller, J. Efficient iterative schemes for ab initio total-energy calculations using a plane-wave basis set. *Physical review B* **1996**, *54*, 11169.
- (54) Perdew, J. P.; Burke, K.; Ernzerhof, M. Generalized gradient approximation made simple. *Physical review letters* **1996**, *77*, 3865.
- (55) Hedin, L. New method for calculating the one-particle Green's function with application to the electron-gas problem. *Physical Review* **1965**, *139*, A796.
- (56) Togo, A.; Oba, F.; Tanaka, I. First-principles calculations of the ferroelastic transition between rutile-type and CaCl₂-type SiO₂ at high pressures. *Physical Review B* **2008**, *78*, 134106.

- (57) Togo, A.; Tanaka, I. First principles phonon calculations in materials science. *Scripta Materialia* **2015**, *108*, 1–5.
- (58) Giannozzi, P.; Baroni, S.; Bonini, N.; Calandra, M.; Car, R.; Cavazzoni, C.; Ceresoli, D.; Chiarotti, G. L.; Cococcioni, M.; Dabo, I. et al. QUANTUM ESPRESSO: a modular and open-source software project for quantum simulations of materials. *Journal of physics: Condensed matter* **2009**, *21*, 395502.
- (59) Mostofi, A. A.; Yates, J. R.; Lee, Y.-S.; Souza, I.; Vanderbilt, D.; Marzari, N. wannier90: A tool for obtaining maximally-localised Wannier functions. *Computer physics communications* **2008**, *178*, 685–699.
- (60) Wu, Q.; Zhang, S.; Song, H.-F.; Troyer, M.; Soluyanov, A. A. WannierTools: An open-source software package for novel topological materials. *Computer Physics Communications* **2018**, *224*, 405–416.